IOP Concise Physics

Fourier Ptychographic Imaging

A MATLAB® tutorial

Guoan Zheng

Chapter 1

Basic concepts in Fourier optics

In this chapter, we will briefly review the basic concepts in Fourier optics. The operation of conventional imaging systems can be modeled by two steps, as shown in figure 1.1: 1) the low-pass filtering process of the imaging system, and 2) the discrete sampling process of the image sensor.

In step 1, the employed optical system acts like a low-pass filter, with a cutoff frequency determined by the numerical aperture (NA) of the lens. Only the spatial-frequency components within the passband can be collected by the optical system and form an image at the detector plane. Such a low-pass filtering process imposes a resolution limit on the imaging platform. For coherent imaging, the resolution limit for the complex light field is λ/NA, where λ is the wavelength of the incident light. For incoherent imaging, the resolution limit for the intensity signal is $\lambda/(2\text{NA})$.

In step 2, the light signal is sampled by the image sensor. The pixel size of the image sensor needs to satisfy the Nyquist limit, i.e., at least two samples are made for the smallest feature of the signal. If the pixel size of the image sensor is too large, it would introduce the aliasing problem to the final captured image, as shown in figure 1.1 (bottom right). A smaller pixel size of the image sensor helps to address the aliasing problem; however, it may also impose limitations on the dynamic range and the signal-to-noise ratio of the sensor chip.

In the following, we will discuss the coherent and incoherent imaging systems from the transfer-function point of view. We will also discuss how to model optical aberrations in imaging systems. Materials in this chapter are useful for understanding the concept of Fourier ptychography (FP). The interested reader can also refer to [1–3] for more details on Fourier optics.

1.1 Coherent imaging system

We first consider a coherent imaging system where a spatially coherent light source is used for sample illumination (we will refer to it as coherent illumination in the future). Under coherent illumination condition, the phasor amplitudes of the light

doi:10.1088/978-1-6817-4273-1ch1

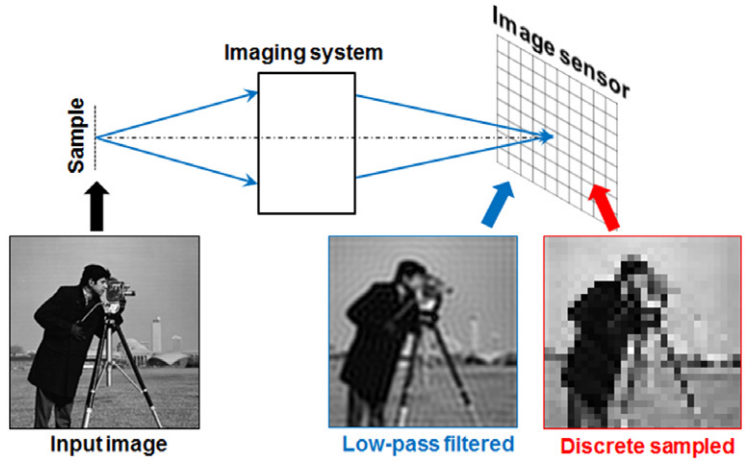

Figure 1.1. The operation of conventional imaging systems. The light field from the object (bottom left) is low-pass filtered by the imaging system (bottom middle) and discretely sampled by the image sensor (bottom right).

field vary in unison at all spatial points. Therefore, a coherent imaging system is linear in complex amplitude:

$$A_{\text{output}}(x, y) = h(x, y) \otimes A_{\text{input}}(x, y) \tag{1.1}$$

In equation (1.1), A_{input} and A_{output} represent the input and output complex amplitudes of the light field, $h(x, y)$ represents the coherent point spread function in the spatial domain, and '$\otimes$' represents 2D convolution. We can transform equation (1.1) to the spatial-frequency (Fourier) domain and obtain:

$$G_{\text{coh\_output}}\left(k_x, k_y\right) = H_{\text{coh}}\left(k_x, k_y\right) G_{\text{coh\_input}}\left(k_x, k_y\right) \tag{1.2}$$

In equation (1.2), $G_{\text{coh\_input}}$ and $G_{\text{coh\_output}}$ represent the input and output Fourier spectrums of the complex amplitudes. $H_{\text{coh}}(k_x, k_y)$ is the Fourier transform of $h(x, y)$ and it is commonly referred to as coherent transfer function.

Coherent illumination condition can be obtained when the light waves come from a single point source. The common light sources for coherent illumination are laser diodes and spatially-confined LEDs. We can also add a small pinhole in front of an extended light source to obtain the coherent illumination condition (the pinhole can be treated as a single point source in this case). In this case, however, the achievable brightness would be much weaker than the case of laser diode. Strictly speaking, there is no real point source for coherent illumination; even for laser diode, the light emitting area has a certain size. Rigorous treatment of the coherent illumination condition is beyond the scope of this book. The interested reader can refer to the theory of partial coherence in [2].

To simulate the imaging process of a coherent imaging system, we consider a microscope example with a 1× magnification, 0.2 NA objective lens. The incident wavelength is 0.5 μm and the final image is sampled by an image sensor with a 0.5 μm pixel size. In the following, we will first create a high-resolution input object

(lines 1–4) and set up the coherent imaging system (lines 5–9). We will then simulate the low-pass filtering process of the imaging system (lines 10–21). Finally, we will obtain the output complex amplitude and intensity images of the simulated object (lines 22–26).

```
1   %% simulate a high-resolution object
2   objectIntensity = double(imread('cameraman.tif'));
3   objectAmplitude = sqrt(objectIntensity);
4   imshow(objectAmptitude,[]);title('Input object (amplitude)');
5   %% set up the parameters for the coherent imaging system
6   waveLength = 0.5e-6;
7   k0=2*pi/waveLength;
8   pixelSize = 0.5e-6;
9   NA = 0.1; cutoffFrequence = NA*k0;
10   %% set up the low-pass filter
11   objectAmptitudeFT=fftshift(fft2(objectAmptitude));
12   [m n]=size(objectAmptitude);
13   kx=-pi/pixelSize:2*pi/(pixelSize*(n-1)):pi/pixelSize;
14   ky=-pi/pixelSize:2*pi/(pixelSize*(n-1)):pi/pixelSize;
15   [kxm kym]=meshgrid(kx,ky);
16   CTF=((kxm.^2+kym.^2)<cutoffFrequency^2); % the coherent transfer function
17   imshow(CTF,[]);title('CTF in the spatial frequency domain');
18   %% the filtering process
19   outputFT=CTF.*objectAmptitudeFT;
20   imshow(log(abs(outputFT)),[]);
21   title('Filtered spectrum in the spatial frequency domain');
22   %% output amplitude and intensity
23   outputAmplitude = ifft2(ifftshift(outputFT));
24   outputIntensity = abs(outputAmplitude).^2;
25   figure;imshow(outputAmplitude,[]);
26   title('Output object (amplitude)');
```

In line 2, we simulate a high-resolution intensity object. We assume the phase of the object is a constant and we convert the intensity to complex amplitude in line 3. In lines 5–9, we set up the parameters for the coherent imaging system. In particular, we define the wave number in line 7 and the cutoff frequency in line 9. In lines 11–17, we set up the low-pass filter (i.e. the coherent transfer function) in the spatial-frequency domain. The low-pass filtering process is performed in line 19, where we transform the object's complex amplitude to the spatial-frequency domain using fast Fourier transform and multiply it with the coherent transfer function. The filtered spectrum is then transformed back to the spatial domain using the inverse fast Fourier transform in line 23. The final output amplitude and intensity can be obtained in lines 23 and 24.

The results of this simulation study are shown in figure 1.2, where we compare the input and output amplitude in both the spatial and spatial-frequency domains (spatial-frequency domain will be referred to as Fourier domain in the future). We note that, a coherent imaging system is linear in complex amplitude, and thus, the filtering process in line 19 is for the complex amplitude of the light field, not the intensity. Once we obtain the output complex amplitude, we can convert it back to intensity, as shown in line 24. We also note that, conventional image sensors can only detect light intensity; the complex phase information is lost in the measuring process. In order to detect the complex amplitude information, we can use phase retrieval [4–12] or holographic approaches [13–15] to recover the lost phase information from intensity measurements. In particular, Fourier ptychography is

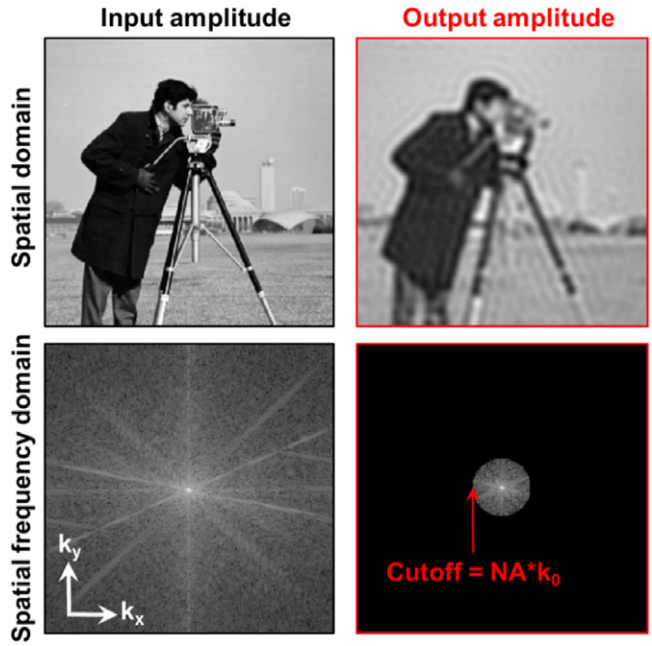

Figure 1.2. The low-pass filtering process of a coherent imaging system.

a coherent phase-retrieval approach. In the recovery process of FP, the acquired intensity images under different incident angles are used to recover the complex amplitude of the object and improve the resolution beyond the cutoff frequency of the employed optics [16].

1.2 Incoherent imaging system

In a coherent imaging system, the illumination light waves come from a point source and the phasor amplitudes of the light waves vary in unison at all spatial points. Here, we consider another illumination condition with the opposite property such that the phasor amplitudes at different points vary in a totally uncorrelated manner. Such an illumination condition is called spatially incoherent (we will simply refer to it as incoherent in the future). The most common example for incoherent imaging is the Köhler illumination in microscope settings, where samples are illuminated by uncorrelated plane waves from different incident angles.

For an incoherent imaging system, the impulse responses at different spatial points vary in an uncorrelated manner. As such, they must be added on an intensity basis instead of the complex amplitude basis. It follows that an incoherent imaging system is linear in intensity and the point spread function is the squared magnitude of the coherent point spread function:

$$I_{\text{output}}(x, y) = |h(x, y)|^2 \otimes I_{\text{input}}(x, y) \tag{1.3}$$

In equation (1.3), I_{input} and I_{output} represent the input and output intensity images, and $h(x, y)$ is the coherent point spread function in the spatial domain. The impulse

response $|h(k_x, k_y)|^2$ is commonly known as incoherent point spread function. We can also transform equation (1.3) to the Fourier domain and obtain:

$$G_{\text{incoh\_output}}(k_x, k_y) = H_{\text{incoh}}(k_x, k_y) G_{\text{incoh\_input}}(k_x, k_y) \tag{1.4}$$

In equation (1.4), $G_{\text{incoh\_input}}$ and $G_{\text{incoh\_output}}$ represent the input and output Fourier spectrums of the intensity images, and $H(k_x, k_y)$ is the Fourier transform of $|h(x, y)|^2$ and known as incoherent transfer function.

In the following, we will use the same microscope imaging example (1× magnification, 0.1 NA objective lens, 0.5 μm wavelength, and 0.5 μm pixel size) to demonstrate the incoherent imaging process. The key idea of this simulation is to generate the incoherent transfer function and perform the low-pass filtering process in the Fourier domain.

```
1   %% simulate an incoherent imaging system
2   objectIntensity=double(imread('cameraman.tif'));
3   imshow(objectIntensity,[]);title('Input object (intensity)');
4   %% set up the parameters for the coherent imaging system
5   waveLength = 0.5e-6;
6   k0=2*pi/waveLength;
7   pixelSize = 0.5e-6;
8   NA = 0.1;
9   cutoffFrequency = NA*k0;
10  %% set up the coherent transfer function in the Fourier domain
11  objectIntensityFT=fftshift(fft2(objectIntensity));
12  [m n]=size(objectIntensity);
13  kx=-pi/pixelSize:2*pi/(pixelSize*(n-1)):pi/pixelSize;
14  ky=-pi/pixelSize:2*pi/(pixelSize*(n-1)):pi/pixelSize;
15  [kxm kym]=meshgrid(kx,ky);
16  CTF=((kxm.^2+kym.^2)<cutoffFrequency^2); % pupil function circ(kmax)
17  imshow(CTF,[]);title('Coherent transfer function in the Fourier domain');
18  %% set up the incoherent transfer function
19  cpsf=fftshift(ifft2(ifftshift(CTF))); % coherent PSF
20  ipsf=(abs(cpsf)).^2; % incoherent PSF
21  OTF=abs(fftshift(fft2(ifftshift(ipsf)))); % incoherent transfer function
22  OTF=OTF./max(max(OTF));
23  figure;imshow(abs(OTF),[]);
24  title('Incoherent transfer function in the Fourier domain');
25  %% perform low-pass filtering and generate the output intensity image
26  outputFT=OTF.*objectIntensityFT;
27  imshow(log(abs(objectIntensityFT)),[]);
28  title('Filtered spectrum in the Fourier domain');
29  outputIntensity = ifft2(ifftshift(outputFT));
30  figure;imshow(outputIntensity,[]);title('Output object (intensity)');
```

Similar to the coherent imaging case, we generate the coherent transfer function in line 16. We then transform the coherent transfer function to the spatial domain and obtain the coherent point spread function in line 19. Next, we take the squared magnitude of the coherent point spread function to obtain the incoherent point spread function in line 20. Finally, we transform the incoherent point spread function back to the Fourier domain to obtain the incoherent transfer function in line 21. The low-pass filtering process is performed in line 26, similar to the case of coherent imaging. The final low-pass filtered intensity output is obtained in line 29 and it is shown in figure 1.3.

Figure 1.4 shows the comparison between the coherent and incoherent transfer functions. We can see that the cutoff frequency of the incoherent transfer function is

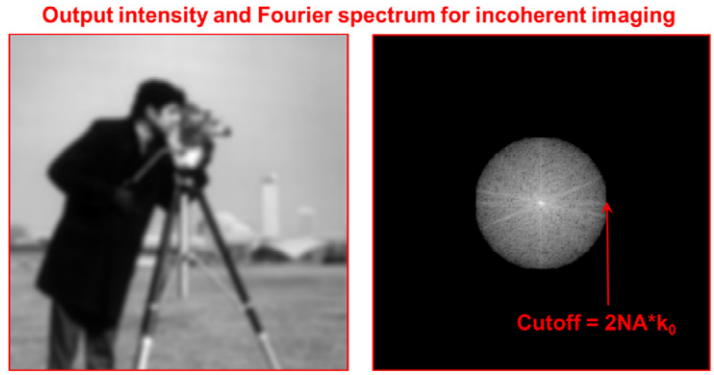

Figure 1.3. The simulated output intensity and Fourier spectrum in an incoherent imaging setting.

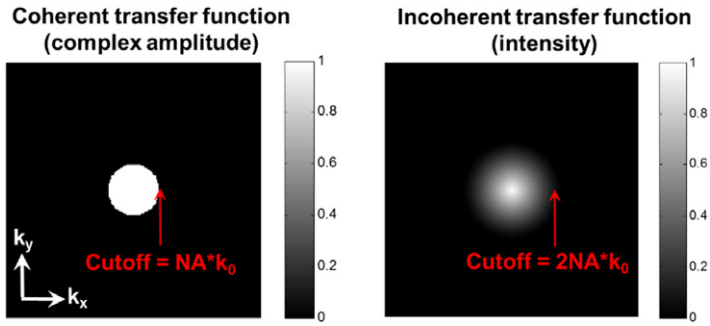

Figure 1.4. The comparison between the coherent and incoherent transfer functions.

twice the cutoff frequency of the coherent transfer function. However, it does not follow that incoherent illumination yields a better resolution than coherent illumination, as we are comparing image intensity to complex amplitude. In fact, which type of illumination is better strongly depends on the sample property, and in particular on the phase distribution of the object. The interested reader can refer to chapter 6 in [1] for more details.

1.3 Modeling aberrations

In previous sections, we assume the imaging system does not contain any optical aberration. Such a system is called a diffraction-limited system, where the achievable resolution is only determined by the NA. We now consider the effect of optical aberration, which imposes practical limits on resolution performance. In particular, we will model the aberrations using the transfer-function approach. We note that, a treatment of various types of aberrations and their effects on frequency response is beyond the scope of this chapter. The interested reader can refer to, for example, [17].

To model aberrations in the imaging process, we can simply introduce a phase term in the coherent transfer function (CTF) as follows:

$$\mathrm{CTF}\left(k_x, k_y\right) = \mathrm{circ}(NA \cdot k_0) \cdot \mathrm{e}^{\mathrm{i} \cdot W\left(k_x, k_y\right)}, \tag{1.5}$$

where the circle function 'circ' generates a circular mask with a radius of $\mathrm{NA} \cdot k_0$, and $\mathrm{W}(k_x, k_y)$ represents the wavefront aberration of the system. We can further decompose the wavefront aberration into a summation of different Zernike modes $\mathrm{Z}(m, n)$ as follows:

$$\mathrm{W}\left(k_x, k_y\right) = \sum a_{(m,n)} \mathrm{Z}(m, n), \tag{1.6}$$

where $a_{(m,n)}$ represents the coefficient for the Zernike mode $\mathrm{Z}(m, n)$. As an example, we have the second-order defocus aberration $\mathrm{W}(k_x, k_y) = a_{(2,0)}\mathrm{Z}(2, 0)$, where $a_{(2,0)}$ represents the amount of defocus aberration. Similarly, $a_{(2,2)}$ and $a_{(2,-2)}$ represent the amounts of second-order astigmatism aberrations along two directions; $a_{(3,1)}$ and $a_{(3,-1)}$ represent the amounts of third-order coma aberrations along two directions; $a_{(4,0)}$ represents the amount of fourth-order spherical aberration. In short, equations (1.5) and (1.6) provide a means to model different aberrations in the imaging process. In the simulation code, we only need to add the following lines to model them in the coherent transfer function:

```
1  W = 2*gzn(pixelNumber,pixelNumberAperture,2,0)+
       4*gzn(pixelNumber,pixelNumberAperture,4,0);
2  CTF=exp(1i.*W).*((kxm.^2+kym.^2)<cutoffFrequency^2);
3  imshow(angle(CTF),[]);title('Coherent transfer function with aberrations');
```

In line 1, we model the wavefront aberration $\mathrm{W}(k_x, k_y)$ as the summation of the second-order defocus and the fourth-order spherical aberrations. We use the 'gzn' function to generate different Zernike modes (similar Zernike functions can be found on the MATLAB File Exchange site). This function takes four parameters from left to right: the width of the input image, the diameter of the pupil aperture, and the two indexes of the Zernike mode. In particular, we have $a_{(2,0)} = 2$ and $a_{(4,0)} = 4$ in the simulation code. In line 2, we model the coherent transfer function using equation (1.5). Once we get the coherent transfer function with aberrations, we can use the coherent imaging procedures in section 1.1 to obtain the output complex amplitude.

To model aberrations in an incoherent imaging system, we need to convert the coherent transfer function (with aberrations) to the incoherent transfer function using the procedures in section 1.2. We can then apply the incoherent transfer function in the filtering process to generate the output intensity image. In figure 1.5, we show two different aberrations in the Fourier domain and their corresponding coherent and incoherent outputs. We can see that the achievable resolution degrades when wavefront aberrations are presented in the imaging system.

Aberration plays a critical role in the design of an imaging platform. As an example, a conventional microscope has a tradeoff between resolution and field of view. A better resolution usually implies a smaller field of view, limiting the imaging throughput of the microscope platform. The tradeoff between resolution and field of view, in fact, comes from aberrations of the objective lens. The common strategy to expand the field of view is to scale up the lens's size [18]. However, simple

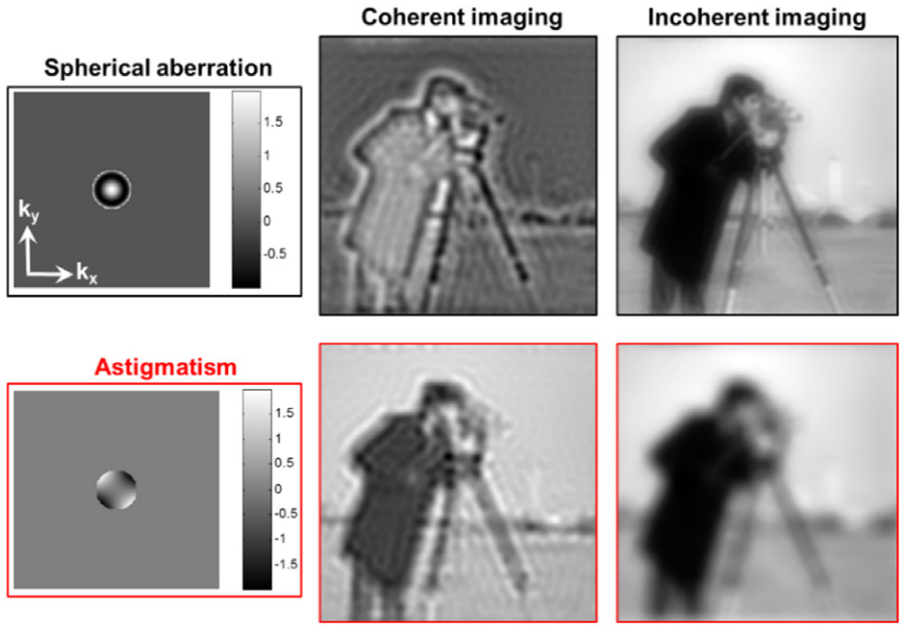

Figure 1.5. Modeling aberrations in the coherent and incoherent imaging systems. Top row: the simulated coherent and incoherent images with spherical aberration ($a_{(4,0)}$= 2). Bottom row: the simulated coherent and incoherent images with astigmatism aberration ($a_{(2,2)}$= 4).

size-scaling would introduce aberrations to the system. To compensate for these aberrations, we need to introduce more optical surfaces to increase the degrees of freedom in lens optimization. With the optomechanical constraints of a conventional microscope platform, expanding field of view without compromising the achievable resolution is considered very challenging in the design of high-resolution objective lenses.

Bibliography

[1] Goodman J W 2005 *Introduction to Fourier optics* (Austin, TX: Roberts and Company)
[2] Goodman J W 2015 *Statistical optics* (Wiley: New York)
[3] Voelz D G 2011 *Computational fourier optics: a MATLAB tutorial* (Bellingham, WA: SPIE Optical Engineering Press)
[4] Fienup J R 1982 Phase retrieval algorithms: a comparison *Appl. Opt.* **21** 2758–69
[5] Elser V 2003 Phase retrieval by iterated projections *JOSA A* **20** 40–55
[6] Faulkner H M L and Rodenburg J M 2004 Movable aperture lensless transmission microscopy: A novel phase retrieval algorithm *Phys. Rev. Lett.* **93** 023903
[7] Maiden A M and Rodenburg J M 2009 An improved ptychographical phase retrieval algorithm for diffractive imaging *Ultramicroscopy* **109** 1256–62
[8] Gonsalves R 1976 Phase retrieval from modulus data *JOSA* **66** 961–4
[9] Fienup J R 1987 Reconstruction of a complex-valued object from the modulus of its Fourier transform using a support constraint *JOSA A* **4** 118–23

[10] Candes E J, Strohmer T and Voroninski V 2013 Phaselift: Exact and stable signal recovery from magnitude measurements via convex programming *Comm. Pure Appl. Math.* **66** 1241–74
[11] Candes E J, Eldar Y C, Strohmer T and Voroninski V 2015 Phase retrieval via matrix completion *SIAM Review* **57** 225–51
[12] Waldspurger I, d'Aspremont A and Mallat S 2015 Phase recovery, maxcut and complex semidefinite programming *Math. Program.* **149** 47–81
[13] Schnars U and Jueptner W 2005 *Digital Holography* (Berlin: Springer)
[14] Cuche E, Marquet P and Depeursinge C 2000 Spatial filtering for zero-order and twin-image elimination in digital off-axis holography *Appl. Opt.* **39** 4070–75
[15] Yamaguchi I and Zhang T 1997 Phase-shifting digital Holography *Opt. Lett.* **22** 1268–70
[16] Zheng G, Horstmeyer R and Yang C 2013 Wide-field, high-resolution Fourier ptychographic microscopy *Nature Photonics* **7** 739–45
[17] Williams C S and Becklund O A 1989 *Introduction to the optical transfer function* vol. 112 (Bellingham, WA: SPIE Optical Engineering Press)
[18] Lohmann A W 1989 Scaling laws for lens systems *Appl. Opt.* **28** 4996–98